Inflammation: Basic Principles and Clinical Correlates, J. I. Gallin, I. M. Goldstein, R. Snyderman, Eds. (Raven, New York, 1988), p. 309.
7. C. Volker *et al.*, *J. Biol. Chem.* **266**, 21515 (1991).
8. P. S. Backlund and R. R. Aksamit, *ibid.* **263**, 15864 (1988); P. S. Backlund, *ibid.* **267**, 18432 (1992).
9. A. Huzoor-Akbar, D. A. Winegar, E. G. Lapetina, *ibid.* **266**, 4387 (1991).
10. C. Volker, R. A. Miller, J. B. Stock, *Methods* **1**, 283 (1990).
11. C. A. Hrycyna and S. Clarke, *Mol. Cell. Biol.* **10**, 5071 (1990); R. C. Stephenson and S. Clarke, *J. Biol. Chem.* **265**, 16248 (1990); *ibid.* **267**, 13314 (1992).
12. A. Abo *et al.*, *Nature* **353**, 668 (1991); U. G. Knaus, P. G. Heyworth, T. Evans, J. T. Curnutte, G. M. Bokoch, *Science* **254**, 1512 (1991); D. Rotrosen, C. L. Yeung, T. L. Leto, H. L. Malech, C. H. Kwong, *ibid.* **256**, 1459 (1992).
13. R. F. O'Dea *et al.*, *Nature* **272**, 462 (1978).
14. H. M. Korchak, L. E. Rutherford, G. Weissmann, *J. Biol. Chem.* **259**, 4070 (1984); J. Reibman *et al.*, *ibid.* **263**, 6322 (1988).
15. G. M. Bokoch and L. A. Quilliam, *Biochem. J.* **267**, 407 (1990); M. Kawata *et al.*, *Proc. Natl. Acad. Sci. U.S.A.* **87**, 8960 (1990); J. Didsbury, R. F. Weber, G. M. Bokoch, T. Evans, R. Snyderman, *J. Biol. Chem.* **264**, 16378 (1989); B. T. Kinsella, R. A. Erdman, W. A. Maltese, *ibid.* **266**, 9786 (1991); I. Maridonneau-Parini, C. Yang, M. Bornens, B. Goud, *J. Clin. Invest.* **87**, 901 (1991); C. C. Farnsworth *et al.*, *Proc. Natl. Acad. Sci. U.S.A.* **88**, 6196 (1991).
16. C. Volker, P. Lane, C. Kwee, M. Johnson, J. B. Stock, *FEBS Lett.* **295**, 189 (1991).
17. E. A. Eklund, M. Marshall, J. B. Gibbs, C. D. Crean, T. G. Gabig, *J. Biol. Chem.* **266**, 13964 (1991).
18. Y. Hori *et al.*, *Oncogene* **6**, 515 (1991).
19. M. Isomura, A. Kikuchi, N. Ohga, Y. Takai, *ibid.*, p. 119.
20. M. S. Springer, M. F. Goy, J. Adler, *Nature* **280**, 279 (1979); J. B. Stock, G. S. Lukat, A. M. Stock, *Annu. Rev. Biophys. Biophys. Chem.* **20**, 109 (1991).
21. M. C. Pike, N. M. Kredich, R. Snyderman, *Proc. Natl. Acad. Sci. U.S.A.* **75**, 3928 (1978).
22. J. B. Stock, S. Clarke, D. E. Koshland, *Methods Enzymol.* **106**, 310 (1984).
23. M. R. Philips *et al.*, *J. Biol. Chem.* **266**, 1289 (1991).
24. I. M. Goldstein, M. Cerquiera, S. Lind, H. B. Kaplan, *J. Clin. Invest.* **59**, 249 (1977).
25. We thank D. Sabatini for helpful discussions and D. Rotrosen and E. Lapetina for supplying antisera. We are grateful to A. Feoktistov and S. Muscat for technical assistance and to A. Cody and J. McMenamin-Balano for assistance in preparing the manuscript. M.R.P. is supported by grants from the National and New York chapters of the Arthritis Foundation. M.H.P. is a fellow of the New York chapter of the Arthritis Foundation and is supported by an NIH training grant to G.W. (AR-O7176-18). C.V. is supported by a fellowship from the NIH (GM-8309). M.G.R. is supported by a grant from the NIH (GM 20277). G.W. is supported by grants from the NIH (AR-11949-25 and HL-19721-16). J.B.S. is supported by grants from the NIH (AI-20980) and the American Cancer Society (MN-486).

16 September 1992; accepted 25 November 1992

Altered Prevalence of Gating Modes in Neurotransmitter Inhibition of N-Type Calcium Channels

Anne H. Delcour* and Richard W. Tsien†

G protein–mediated inhibition of voltage-activated calcium channels by neurotransmitters has important consequences for the control of synaptic strength. Single-channel recordings of N-type calcium channels in frog sympathetic neurons reveal at least three distinct patterns of gating, designated low-P_o, medium-P_o, and high-P_o modes according to their probability of being open (P_o) at −10 millivolts. The high-P_o mode is responsible for the bulk of divalent cation entry in the absence of neurotransmitter. Norepinephrine greatly decreased the prevalence of high-P_o gating and increased the proportion of time a channel exhibited low-P_o behavior or no activity at all, which thereby reduced the overall current. Directly observed patterns of transition between the various modes suggest that activated G protein alters the balance between modal behaviors that freely interconvert even in the absence of modulatory signaling.

A wide variety of neurotransmitters inhibit high voltage–activated Ca^{2+} channels in vertebrate neurons (*1–6*). At nerve terminals, this diminishes transmitter release and thereby contributes to presynaptic inhibition (*1*) or autoinhibition (*5*). Inhibitory modulation is exemplified by norepinephrine (NE) acting by means of α_2-adrenergic receptors to inhibit N-type channels (*1, 4, 5, 7*). This modulation involves G proteins (*7–10*) acting by a fast, membrane-delimited pathway (*5, 6*), but how this alters the activity of individual Ca^{2+} channels is unclear. On the basis of whole-cell recordings, several hypothetical mechanisms of down-modulation have been proposed: (i) channel block with no change in time- or voltage-dependent kinetics (*1*); (ii) modulation by the addition of an extra nonconducting state with kinetically slow connections to normal gating states (*9, 10*); and (iii) modulation by shifts in the mode of gating, from a "willing" mode, where the channel can be opened by relatively weak depolarizations, to a "reluctant" mode, in which much stronger depolarizations are required (*4, 11, 12*). To test these hypotheses, we examined neurotransmitter modulation of unitary N-type Ca^{2+} channel activity (*5, 13*).

Department of Molecular and Cellular Physiology, Beckman Center, Stanford University Medical Center, Stanford, CA 94305.

*Present address: Department of Biology, University of Houston, Houston, TX 77204.
†To whom correspondence should be addressed.

In the absence of neurotransmitters, N-type Ca^{2+} channels in frog sympathetic neurons exhibit three prominent modes of gating (*13*). When evoked by pulses to a convenient test potential (−10 mV), the gating modes differ widely in their probability of being open (P_o) and are thus classified as high-, medium-, and low-P_o modes (*13*) (Fig. 1, A and B). In the high-P_o mode (Fig. 1A), channel openings are relatively long lasting and closings are short-lived, and P_o at −10 mV is typically ~0.5 or greater. In the medium-P_o mode (Fig. 1B), the openings are somewhat briefer and the closings longer. In the low-P_o mode, the openings are even briefer and the closings even more prolonged.

Figure 1 compares data collected from ten patches with no transmitter present and from ten patches where the patch pipette contained 100 μM NE, a concentration that produces nearly saturating inhibition with little desensitization (*5*). In the presence of NE, the mean patch current was less than half that in the control patches (Fig. 1, insets). Norepinephrine markedly affected the prevalence of high-P_o gating. In the control patches, high-P_o sweeps are represented by a cluster of data points, centered around a mean open duration ($\bar{t}_o$) of ~3 ms and a mean closed time ($\bar{t}_c$) of ~2 ms ($P_o \geq 0.45$). Under the influence of NE, high-P_o gating was largely absent (Fig. 1D).

The near-abolition of high-P_o gating conforms to the proposed NE-induced shift from willing to reluctant gating (*4, 11*). However, even with high-P_o behavior set aside, the gating behavior that remained with NE was far from homogeneous, contrary to predictions of the willing-reluctant hypothesis for maximal neurotransmitter inhibition. The $\bar{t}_o$-$\bar{t}_c$ plot with NE (Fig. 1D) shows a significant negative correlation between $\bar{t}_o$ and $\bar{t}_c$ ($P < 0.001$), which is indicative of more than just one pattern of gating (*14*).

The dominant patterns of gating in the presence of NE are illustrated by the set of consecutive current records in Fig. 2A. Spontaneous switching between two kinds of gating is evident. One pattern, exemplified by sweeps 1 and 2 and 4 to 7, is qualitatively similar to the medium-P_o mode in control recordings (Fig. 1B). Another pattern, typified by sweeps 3 and 8 to 11, resembles low-P_o gating in the control.

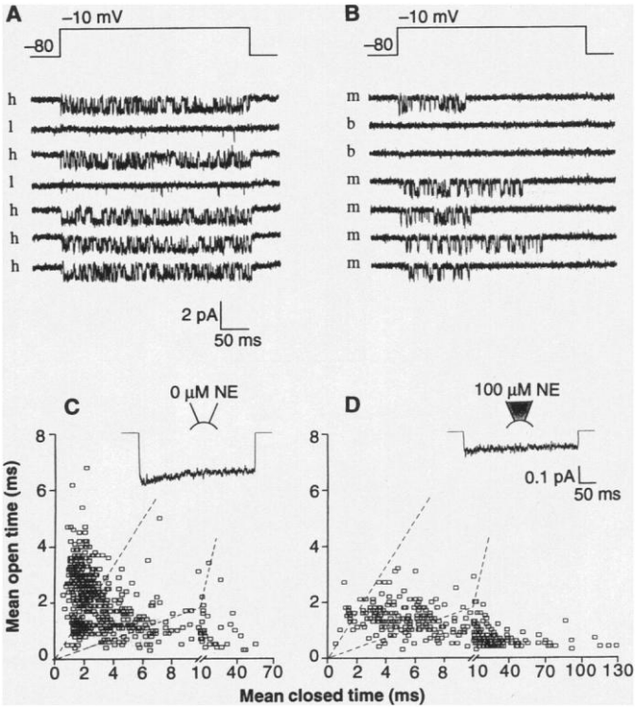

Fig. 1. Multiple gating patterns of N-type Ca^{2+} channels in the absence or presence of neurotransmitter. (**A** and **B**) Representative records from a single control experiment that illustrate the three major gating modes. High-P_o (h) and low-P_o (l) gating modes are interspersed in (A), and medium-P_o gating (m) and blank records (b) are illustrated in (B), with seven consecutive leak-subtracted sweeps in each case. The voltage protocol (top) was a depolarizing pulse from −80 to −10 mV. (**C** and **D**) Gating behavior from ten control experiments (C) and ten patches in the presence of 100 μM NE (D). Each symbol represents the kinetic behavior of an individual sweep with only a single open level; values of mean open time and mean closed time are arithmetic averages calculated for each sweep. Dashed lines correspond to P_o values of 0.45 and 0.15, used to categorize different gating behaviors for later analysis (*13*). (**Insets**) Means of ensemble averages constructed from idealized records for each patch.

The distribution of open durations is shown fitted to a single exponential (Fig. 2B); this fit was significantly inferior to the sum of two exponential components ($P < 0.00001$) (*15*). This points to the existence of at least two distinct open states. Sorting the current records in the presence of NE into low-P_o (Fig. 2C) or medium-P_o (Fig. 2D) groups simplified the kinetic analysis. Once the records were sorted, the individual open duration distributions were both monoexponential, consistent with a classical kinetic scheme for Ca^{2+} channels with only one open state (*16*). The disparity in time constants (τ = 1.13 ms in medium-P_o mode and τ = 0.29 ms in low-P_o mode) reflects a more than threefold difference in exit rates from the open state in the respective modes.

With NE, just as with the control (*13*), distinctions between modes were facilitated by the slowness of intermode switching relative to gating kinetics within a mode. Histograms of the length of apparent sojourns within each mode with NE (Fig. 2, E through G) yielded mean run lengths of 2.97, 2.38, and 1.90 records for blanks and low-P_o and medium-P_o gating, respectively (control values were 2.35, 1.48, and 2.25 records). Because records were taken every 4 s, these run lengths correspond to apparent modal sojourns of several seconds, 10^2- to 10^3-fold longer than a typical cycle of channel opening and closing.

Modulation of divalent cation entry could take place by the alteration of the prevalence of the various modes or by changes in the rapid kinetics within the modes. The collected data show that NE affects the proportion of time that a channel spends in individual modes (Fig. 3A). The proportion of sweeps that displayed high-P_o gating was greatly decreased (3% in the presence of NE versus 32% with the control) ($P < 0.005$), whereas the proportion of records that showed low-P_o gating or no detectable openings (blanks) was increased with NE ($P < 0.05$). On the other hand,the incidence of medium-P_o sweeps was not markedly changed ($P > 0.05$). In contrast to the clear effect of NE on modal weights, the mean values of $\bar{t}_o$ within individual modes were not significantly different in NE or control conditions (Fig. 3B) ($P > 0.05$) (*17*).

The impact of the changes in modal weights on the overall macroscopic current is illustrated in Fig. 3C (*18*). Changes in the relative weights of the modes underlie the dramatic down-modulation. The high-P_o component accounted for about 60% of the total current in the absence of neurotransmitter but made a negligible contribu-

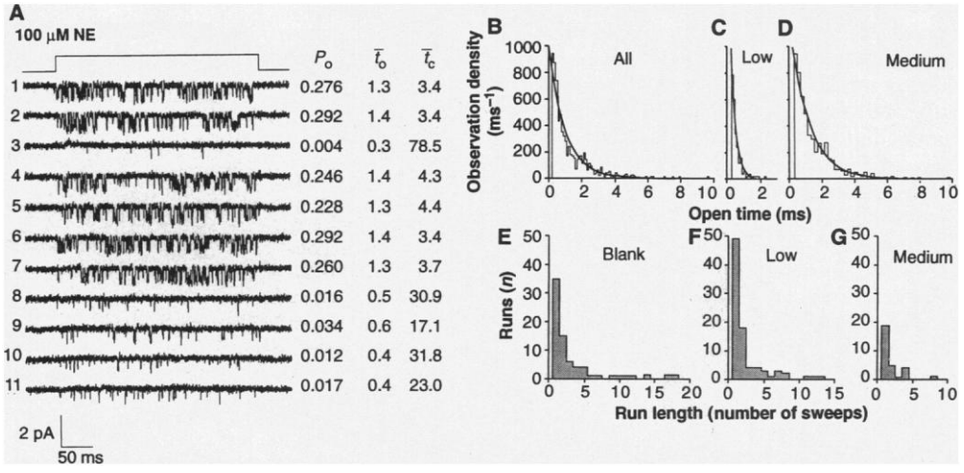

Fig. 2. Two gating modes remain prominent even in the presence of maximally effective concentrations of neurotransmitter. (**A**) Gating behavior observed with 100 μM NE in the patch pipette, illustrated by a series of consecutive unitary current records (left) and associated values (right) of open probability (P_o), mean open time ($\bar{t}_o$), and mean closed time ($\bar{t}_c$) in milliseconds. The same voltage protocol as in Fig. 1, A and B, was used. (**B** through **D**) Distributions of open times collected from the same experiment as in (A). The histogram made from all openings (B) is poorly fitted by a single exponential. However, histograms constructed from sweeps classified as low-P_o (C) or medium-P_o (D) are adequately fitted by single exponentials (τ_{low} = 0.29 ms and τ_{med} = 1.13 ms). The vertical scale in (C) and (D) is half that in (B). (**E** through **G**) Run-length histograms for runs of consecutive sweeps that showed no detectable channel activity (E) or low-P_o (F) or medium-P_o (G) modal behavior. The histograms were constructed from pooled data from ten experiments, with sweeps every 4 s.

tion in the presence of NE. The low-P_o component in the presence of NE was more than doubled relative to the control, but because its absolute contribution was small relative to other components, this was of little consequence. The overall result was a sharp decrease in the total ionic current (*19*).

The participation of low-P_o gating showed up more clearly in the predicted voltage dependence of Ca^{2+} channel activation (Fig. 3D). As the amount of low-P_o behavior increased and that of high-P_o decreased, a greater fraction of the maximal activation required very strong depolarizations. The predicted activation curve with NE shows two distinguishable limbs, consistent with whole-cell tail current measurements (*4*, *11*). The shallowness of the upper limb reflects observed properties of the low-P_o mode (*13*). The voltage dependence of activation of the high-P_o and medium-P_o modes is similar enough to blend together in what would be taken as the willing component.

The binding of G protein subunits to Ca^{2+} channels has been proposed as a mechanism for the down-modulation of N-type currents (*4*, *5*, *9*–*12*). Our observations are consistent with the hypothesis that activated G protein drives the channel from the high-P_o mode to a less active pattern, abbreviating episodes of high-P_o behavior. With large amounts of neurotransmitter (and presumably activated G protein), current records comprised of homogeneous high-P_o activity (Fig. 4A) were extremely rare (<1% of all records). More commonly, high-P_o gating appeared as a transitory epoch along with other gating patterns within an individual sweep (Fig. 4B). The brevity of such epochs seems compatible with the fast kinetics of action of transmitters working via the membrane-delimited pathway (*4*–*6*, *20*–*22*).

G protein–mediated inhibition can be temporarily relieved by a strongly depolarizing prepulse (*4*, *9*–*12*, *23*). Reestablishment of inhibition is G protein–dependent (*10*) and appears as a decay of inward current during a test depolarization after the prepulse (Fig. 4C; *24*). Our cell-attached patch recordings suggest that the decay of whole-cell current ($\tau \sim 30$ ms) arises from transitory sojourns in the high-P_o mode that give way to less active gating. Depolarizing prepulses (9 out of 192 trials) sometimes promoted long-lasting openings near the beginning of the test pulse (Fig. 4D); such openings were never seen when test pulses were not preceded by the strong depolarizations (0 out of 180 trials). The early long openings are consistent with temporary occupation of the high-P_o mode followed by G protein reinhibition and transition to less active modes (*25*, *26*).

These results provide information about the mechanism of neurotransmitter-induced down-modulation. Channel activity was not blocked in an all-or-nothing way but was reduced in a graded fashion through changes in modal prevalence. NE reduced the likelihood of high-P_o gating (but not medium-P_o activity), which thus accounts

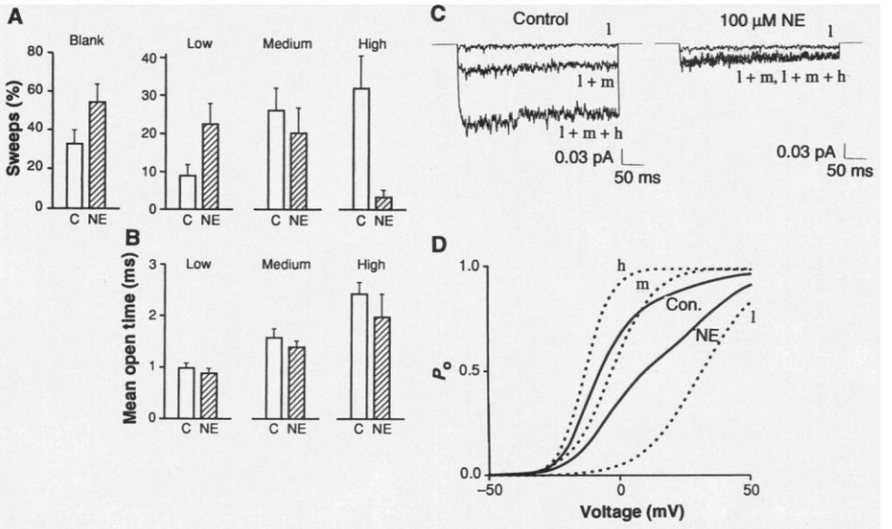

Fig. 3. (**A** and **B**) Neurotransmitter-induced alteration of the balance between modes with no significant change in open time distributions within individual modes. In (A) is the proportion of sweeps in various modes in control patches (C) and in the presence of 100 μM NE. Collected data are represented as mean ± SEM. In (B), $\bar{t}_o$ was averaged across the same set of patches. (**C** and **D**) Altered modal weights can account for N-type channel down-modulation and its voltage dependence. In (C), the contribution of modal components to the overall current is shown in the absence (left) and presence (right) of 100 μM NE. We reconstructed the total current by averaging sweeps within individual modes and then adding up the modal components one at a time (l for low-P_o, m for medium-P_o, and h for high-P_o modes) (*18*). In (D), a reconstruction of voltage (V) dependence of activation for comparison with tail current measurements is shown. Dotted curves show the $P_o(V)$ curves for the individual modes in the form of Boltzmann functions

$$P_o(V) = \{1 + \exp[-(V - V_{1/2})/k]\}^{-1}$$

where the voltage at which P_o is half ($V_{1/2}$) = −13.2, −3.2, and 31 mV and the Boltzmann constant (k) = 5, 7.8, and 11 mV for the low-, medium-, and high-P_o modes, respectively (*13*). Solid curves illustrate the normalized tail activation curves expected in the absence [control (Con.)] and the presence (NE) of 100 μM NE, calculated as the weighted sum of $P_o(V)$ curves [weights are calculated from the mean proportions of (A), normalized to exclude blanks].

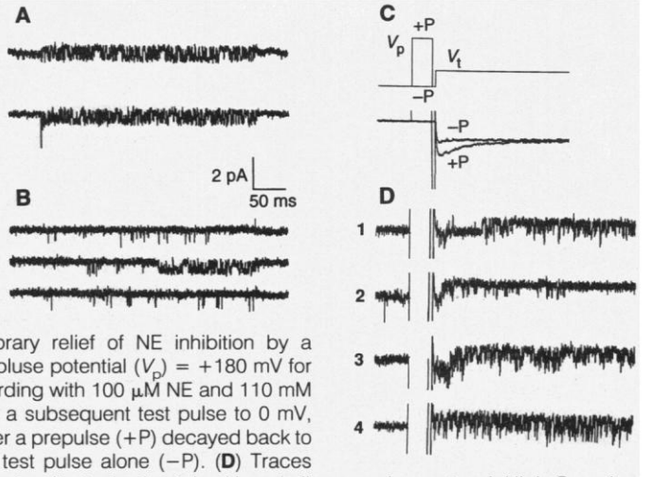

Fig. 4. Properties of residual high-P_o behavior observed in patches exposed to NE. (**A**) Sweeps of high-P_o activity for the full duration of the depolarization (312 ms). (**B**) A short epoch of high-P_o gating amid low-P_o activity in consecutive records from another experiment. For (A) and (B), the voltage protocol is as in Fig. 1A. (**C**) Temporary relief of NE inhibition by a depolarizing prepulse [prepluse potential (V_p) = +180 mV for 40 ms] in a whole-cell recording with 100 μM NE and 110 mM external Ba^{2+} (*24*). During a subsequent test pulse to 0 mV, the extra inward current after a prepulse (+P) decayed back to an amount evoked by the test pulse alone (−P). (**D**) Traces obtained from a multichannel, cell-attached patch with a similar prepulse protocol. High-P_o gating appears in traces 1 to 3 as prolonged openings of one or more channels near the onset of the test pulse to −10 mV that follows a prepulse to +120 mV. Trace 4 is an example of a record that lacks such behavior.

for a substantial (but incomplete) reduction of macroscopic current at moderate test potentials (*1–3*). The retention of low-P_o gating allows nearly full activation of N-type Ca^{2+} conductance by very strong test depolarizations (*4, 11*). These results provide direct evidence for interconversion between modes of gating (*4, 11, 12*), although the observed modal behavior is more complex than merely willing and reluctant, as previously hypothesized.

G proteins might alter the balance between modes in several ways (Fig. 5). The simplest hypothesis is a strictly coupled, sequential model (model A, Fig. 5A). The binding of increasing numbers of G protein subunits (*27*) is tightly linked to displacement of gating toward less active modes (*21*). In a loosely coupled, sequential model (model B, Fig. 5B), the channel may spontaneously interconvert between modes of gating even in the absence of G proteins, but the hierarchy of modes is the same. A third model (model C, Fig. 5C) is akin to a Monod-Wyman-Changeux (MWC) model (*28*). Here, all active modes are interconnected, and the binding of one or more G proteins merely biases the equilibria between modes in favor of low-P_o behavior or no activity.

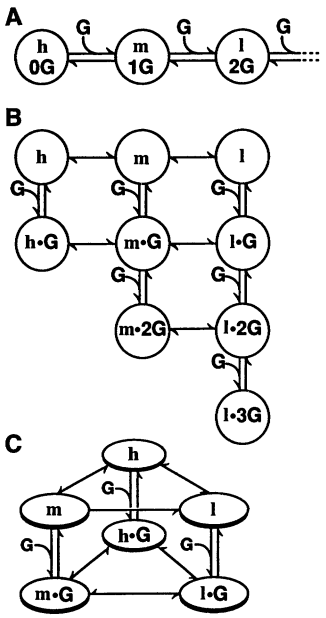

Fig. 5. Alternative kinetic schemes for the effects of G proteins on gating modes. For simplicity, only active modes are depicted. (**A**) Modes arranged in a strict sequence: direct transitions between high-P_o (h) and low-P_o (l) modes are not allowed. Medium-P_o mode, m. The modal transitions are entirely dependent on the binding of one or more G proteins. (**B**) Another model with modes arranged in strict order. Modal transitions can occur even in the absence of G proteins, but direct transitions between high- and low-P_o modes are forbidden. (**C**) MWC model allowing direct modal transitions between all pairs of modes, even in the absence of G protein action. The binding of one (or more) G proteins alters equilibria between modes.

Unitary Ca^{2+} channel recordings permitted tests of these models. Model A predicts that sojourns in the low-P_o mode should be abbreviated as the amount of activated G protein increases (*29*). This is not the case; if anything, the apparent lifetime of the low-P_o mode appeared longer with NE (2.38 records) than with the control (1.48 records). Models A and B both predict that direct modal transitions occur only between adjacent modes: for example, high ⇔ medium and medium ⇔ low. On the contrary, we found high → low and low → high transitions in control patches (Fig. 1A) (*30*) without any sign of intervening sojourns in the medium-P_o mode (*31*). Such transitions also occurred in the presence of NE (Fig. 4B). These results weigh strongly against schemes where the modes are linked in a strictly hierarchical string (model A or B) but would be consistent with model C. Similar hypotheses can be used to explain modal behavior of L-type Ca^{2+} channels and up-modulation by 1,4-dihydropyridines (*32*) or protein kinases (*33*).

The mechanism and kinetics of neurotransmitter-induced inhibition may have important functional consequences for presynaptic inhibition or autoinhibition at nerve terminals. In the sympathetic nervous system, noradrenergic autoinhibition via α_2 receptors may help ensure a more uniform delivery of transmitters to postsynaptic target tissues (*34*). A rapidly developing but slowly decaying inhibition would allow a locally high concentration of NE, released from an individual varicosity, to produce an immediate but lingering inhibitory effect on further release from that varicosity but not at distant sites. It is likely that similar mechanisms contribute in other systems where neurotransmitters control Ca^{2+} entry and presynaptic function.

REFERENCES AND NOTES

1. K. Dunlap and G. Fischbach, *Nature* **276**, 837 (1978); *J. Physiol. (London)* **317**, 519 (1981).
2. For reviews, see R. W. Tsien, D. Lipscombe, V. D. Madison, K. R. Bley, A. P. Fox, *Trends Neurosci.* **11**, 431 (1988); E. Carbone and D. Swandulla, *Prog. Biophys. Mol. Biol.* **54**, 31 (1989); G. Schultz, W. Rosenthal, J. Hescheler, W. Trautwein, *Annu. Rev. Physiol.* **52**, 275 (1990); and R. Anwyl, *Brain Res. Rev.* **16**, 265 (1991).
3. For example, M. Galvan and P. R. Adams, *Brain Res.* **244**, 135 (1982); C. Marchetti, E. Carbone, H. D. Lux, *Pfluegers Arch.* **406**, 104 (1986); E. Wanke *et al.*, *Proc. Natl. Acad. Sci. U.S.A.* **84**, 4313 (1987); R. A. Gross and R. L. Macdonald, *ibid.*, p. 5469; H. Kasai and T. Aosaki, *Pfluegers Arch.* **414**, 415 (1989).
4. B. P. Bean, *Nature* **340**, 153 (1989).
5. D. Lipscombe, S. Kongsamut, R. W. Tsien, *ibid.*, p. 639.
6. P. Forscher, G. S. Oxford, D. Schulz, *J. Physiol. (London)* **379**, 131 (1986); A. Mathie, L. Bernheim, B. Hille, *Neuron* **8**, 907 (1992).
7. M. R. Plummer, A. Rittenhouse, M. Kanevsky, P. Hess, *J. Neurosci.* **11**, 2339 (1991).
8. G. G. Holz IV, S. G. Rane, K. Dunlap, *Nature* **319**, 670 (1986); A. C. Dolphin and R. H. Scott, *J. Physiol. (London)* **386**, 1 (1987); D. A. Ewald, P. C. Sternweis, R. J. Miller, *Proc. Natl. Acad. Sci. U.S.A.* **85**, 3633 (1988); A. C. Dolphin, *Annu. Rev. Physiol.* **52**, 243 (1990).
9. F. Grassi and H. D. Lux, *Neurosci. Lett.* **105**, 113 (1989); C. Marchetti and M. Robello, *Biophys. J.* **56**, 1267 (1989).
10. H. S. Lopez and A. M. Brown, *Neuron* **7**, 1061 (1991).
11. K. S. Elmslie, W. Zhou, S. W. Jones, *ibid.* **5**, 75 (1990); D. J. Beech, L. Bernheim, B. Hille, *ibid.* **8**, 97 (1992).
12. H. Kasai, *J. Physiol. (London)* **448**, 189 (1992).
13. A. H. Delcour, D. Lipscombe, R. W. Tsien, *J. Neurosci.*, in press. Unitary currents were recorded at room temperature (22°C) from cell-attached patches [O. P. Hamill *et al.*, *Pfluegers Arch.* **391**, 85 (1981)]. Pipettes contained solutions of 110 mM $BaCl_2$, 10 mM tetraethyl ammonium (TEA) chloride, 5 mM 4-aminopyridine, and 5 mM Hepes (pH adjusted to 7.3 with TEA-OH) and had resistances of 7 to 15 megohms. The membrane potential was brought to 0 with a bath solution that contained 140 mM potassium aspartate, 10 mM EGTA, 10 mM glucose, 1 mM $MgCl_2$, and 10 mM Hepes (pH adjusted to 7.3 with KOH). Command pulses of 312 ms in duration were delivered every 4 s. The membrane potential of the patch was routinely held at −80 mV, but we occasionally changed it to −40 mV to identify N-type Ca^{2+} channels by their voltage-induced inactivation. Excluded from analysis were patches that displayed L-type channel activity (readily distinguished by unitary conductance and voltage dependence of activation and inactivation). The total number of N-type Ca^{2+} channels in both control and NE patches ranged from one to three. Any NE-dependent changes in the number of functional channels would have little impact on the analysis of open durations, the main focus of this paper, although the interpretation of t_c distributions would be complicated. Analysis of channel kinetics was carried out on sweeps without overlapping openings. Channel openings were detected with the half-amplitude criterion (*16*). For each sweep, $\bar{t}_o$ was calculated as the arithmetic average of all open times and $\bar{t}_c$ as the average of all closed times, excluding the first and last closures during the depolarization. Opening probability P_o was defined for each sweep as $\bar{t}_o/(\bar{t}_o + \bar{t}_c)$. Fits of open time distributions were performed with the maximum likelihood algorithm with the use of a simplex routine.
14. O. McManus and K. M. Magleby, *J. Physiol. (London)* **402**, 79 (1988).
15. The likelihood ratio test was used to determine the number of significant exponential components (*14*).
16. E. Fenwick, A. Marty, E. Neher, *J. Physiol. (London)* **331**, 599 (1982).
17. The only appreciable difference in kinetics was seen in closed times, which appeared longer in the presence of NE than with the control (Fig. 1, C and D). The most likely explanation is that NE promotes an additional pattern of gating, characterized by extremely sparse activity [number of channels × the open probability (NP_o) < 0.01] and very brief openings (t_o < 0.5 ms), analogous to L-type Ca^{2+} channel activity called mode 0_a (*33*). Seen occasionally in control patches (*13*), this pattern is more pronounced with NE. Analysis of t_c and P_o in 0_a was difficult: openings that were clear from visual inspection were often too brief to be detected by the midway crossing criterion (*16*). Thus, for purposes of analysis of runs and modal weights sweeps with NP_o < 0.01 were lumped together with blank records.
18. The total current is reconstructed as

$$I_{total} = A_{low} i_{low} P_{o,low}(t) + A_{med} i_{med} P_{o,med}(t) + A_{high} i_{high} P_{o,high}(t)$$

where I_{total} is the whole-cell current and i is the single-channel current. The modal weighting coefficients (A_{low}, A_{med}, A_{high}) are those plotted in Fig. 3A and allow for the proportion of blank sweeps (A_{blank}). The unitary currents were set at i_{low} = 0.9 pA and i_{med} = i_{high} = 0.7 pA (*13*). We determined the wave form of open probability [$P_o(t)$] for each mode by averaging idealized records for all sweeps falling within the appropriate modal category.
19. The contribution of the medium-P_o mode was only slightly decreased here. In earlier recordings taken under different experimental conditions (*5*), most of the current in control patches was supported by medium-P_o gating, and NE produced a shift away from medium-P_o to low-P_o gating. In either case, the modulation favored a less active mode.
20. S. W. Jones, *Biophys. J.* **60**, 502 (1991).
21. L. M. Boland and B. P. Bean, *J. Neurosci.* **13**, 516 (1993). Boland and Bean propose a quantitative model where a single N-type Ca^{2+} channel can accommodate between zero and four G protein subunits. This would be most consistent with our results if N-type channels displayed four active patterns of gating. Our analysis has separated high-, medium-, and low-P_o gating, but an additional distinction might be made between low-P_o and 0_a-type gating (*33*).
22. With NE, typical sojourns in the high-P_o mode were considerably briefer than the onset time constants of neurotransmitter inhibition, which were ~2 s (*12, 23*). Sojourns in the low-P_o mode were relatively long-lasting, consistent with the slow time constant of recovery from neurotransmitter inhibition, estimated as ~18 s in these cells (*20, 21*).
23. S. R. Ikeda, *J. Physiol.* (*London*) **439**, 181 (1991).
24. In whole-cell recordings (Fig. 4C), pipettes contained a solution with 100 mM CsCl, 10 mM EGTA, 5 mM $MgCl_2$, 2 mM Na adenosine triphosphate, 0.3 mM Na guanosine triphosphate, and 40 mM Hepes (pH 7.3 with CsOH) and had resistances of ~2 megohms. Gigaohm seals and whole-cell configuration were obtained with a bathing solution that contained 120 mM NaCl, 2 mM KCl, 10 mM glucose, and 10 mM Hepes (pH 7.3 with NaOH). For Ba^{2+} current recordings, the bathing solution was changed to one that contained 110 mM $BaCl_2$, 10 mM glucose, 100 nM tetrodotoxin, and 10 mM Hepes (pH 7.3 with TEA-OH).
25. Although it is clear that prepulse-induced sojourns in the high-P_o mode occasionally occurred, more extensive recordings are needed to characterize the kinetics of reinhibition at the unitary level. Our data are limited because the cell-attached patches were often destroyed by the strong prepulses needed to remove the inhibition.
26. Slow relief of inhibition during the test pulse was not seen in our experiments (Fig. 1, insets), which is consistent with its variable occurrence in earlier experiments (*1–12*) depending on the test potential and the type and concentration of neurotransmitter. Slow deinhibition might not be expected under the experimental conditions used for the unitary recordings. The high NE concentration was chosen for a near-maximal degree of inhibition but would be expected to increase the amount of activated G proteins and thereby minimize the time-dependent relief of inhibition (*4, 9–11*). We chose relatively weak test depolarizations to keep unitary current large and to reduce open probability in the low-P_o mode so that this activity would be easily distinguished from other modes; however, this would also hamper relief of inhibition, because channel opening in the reluctant mode is needed to drive off the inhibitory G protein (*4, 11*).
27. Y. Kurachi, H. Ito, T. Sugimoto, *Pfluegers Arch.* **416**, 216 (1990).
28. J. Monod, J. Wyman, J.-P. Changeux, *J. Mol. Biol.* **12**, 88 (1965).
29. In model A, the transition rate from low → (blank/0_a) should increase with the amount of activated G protein.
30. Here, transitions between the high-P_o and the low-P_o modes were the most relevant because blank sweeps may reflect either G protein–mediated inhibition or merely inactivation. Figure 1A exemplifies a total of 13 high → low and 9 low → high transitions out of a total of 888 sweeps in control patches.
31. Some intermediary sojourns in the medium-P_o mode might be brief enough to go undetected, but this is highly unlikely in four consecutive instances because the apparent lifetime of medium-P_o mode gating was relatively long (two and a half sweeps in the patch in Fig. 1, A and B).
32. P. Hess, J. B. Lansman, R. W. Tsien, *Nature* **311**, 538 (1984); T. N. Marks and S. W. Jones, *J. Gen. Physiol.* **99**, 367 (1992).
33. D. T. Yue, S. Herzig, E. Marban, *Proc. Natl. Acad. Sci. U.S.A.* **87**, 753 (1990).
34. J. A. Bevan, F. M. Tayo, R. A. Rowan, R. D. Bevan, *Fed. Proc.* **43**, 1365 (1984).
35. We are grateful to D. Lipscombe for her participation in the early stages of this project. We thank R. W. Aldrich, D. D. Friel, W. A. Sather, R. H. Scheller, J. Yang, and J.-F. Zhang for their comments on the manuscript, K. Bley and P. Rivas for help in preliminary experiments, and R. W. Aldrich for suggesting the model in Fig. 5B. This work was supported by a National Research Service Award (A.H.D.), Public Health Service grants NS24607 and HL13156, and the Silvio Conte Center of the National Institute of Mental Health at Stanford University.

24 August 1992; accepted 1 December 1992

Shutdown of Class Switch Recombination by Deletion of a Switch Region Control Element

Steffen Jung,* Klaus Rajewsky, Andreas Radbruch

Upon activation, B lymphocytes can change the class of the antibody they express by immunoglobulin class switch recombination. Cytokines can direct this recombination to distinct classes by the specific activation of repetitive recombinogenic DNA sequences, the switch regions. Recombination to a particular switch region ($s_\gamma1$) was abolished in mice that were altered to lack sequences that are 5′ to the $s_\gamma1$ region. This result directly implicates the functional importance of 5′ switch region flanking sequences in the control of class switch recombination. Mutant mice exhibit a selective agammaglobulinemia and may be useful in the assessment of the biological importance of immunoglobulin G1.

Immunoglobulin class switch recombination permits a B cell to sequentially express antibodies that have identical specificities but that differ in class and thus effector function. This recombination, which moves the variable region exon of the immunoglobulin heavy (IgH) chain to associate with a different set of constant region exons, is mediated by switch (s) regions—that is, arrays of short tandem repeats located upstream of each constant region (C_H) gene segment, except C_δ. Once activated, class switch recombination is a regulated process, directed to the same switch region on the active and the allelically excluded, inactive allele of a given B cell (*1*). Class switching is directed by cytokines. For example, the addition of interleukin-4 (IL-4) to cultures of polyclonally activated B cells induces switching to IgG1 and IgE (*2*). The direction of class switching may be determined by the modulation of accessibility of the individual switch regions to a common switch recombinase (*3*). Before recombination, 5′ switch region flanking sequences are subjected to cytokine-induced demethylation (*4*) and chromatin changes (*5*). Furthermore, the activation of promoter and enhancer elements in these regions leads to transcription of the respective unrearranged (germline) switch regions and their associated C_H genes (*6*). Despite the large body of correlative evidence for germline transcription and class switch recombination (*3, 6*), a functional relation between switch region flanking sequences and class switch recombination has not been directly shown.

To test the functional importance of switch region flanking sequences for switch recombination, we generated mutant mice that lack 5′ flanking sequences of the $s_\gamma1$ switch region (*7*) (Fig. 1). The homologous recombination event yields an IgH locus with the 5′ $s_\gamma1$ region being replaced by an inversely oriented neomycin resistance (*neo*^{r}) gene needed for selection of recombinants in the conventional targeting scheme (*8*). In the targeting construct (*9*), the *neo*^{r}-cassette replaces 1.7 kb of the 5′ $s_\gamma1$ region spanning all sites of molecular changes known to be induced by the cytokine IL-4—that is, a protein binding site (*10*), deoxyribonuclease (DNase) I hypersensitive sites (*5*), sites of specific demethylation (*4*), and the promoter elements and splice donor site of the $I_\gamma1$-germline transcript (*11*) (Fig. 1D).

Using a murine embryonic stem (ES) cell line derived from 129/Ola mice (*IgH*^{a}), we generated ES cell clones that were heterozygous for the targeted replacement of the 5′ $s_\gamma1$ region (designated neoΔ5′$s_\gamma1$) by homologous recombination (*12*). To exclude the influence of the *neo*^{r} gene or its control

Institute for Genetics, University of Cologne, D-5000 Cologne 41, Germany.

*To whom correspondence should be addressed.